Tape-Spring Rolling Hinges

Alan M. Watt[1] and Sergio Pellegrino[2]

Abstract

This paper presents a new design of a low cost, unlubricated, self-deploying, self-locking hinge whose properties can be easily modified to meet different requirements. A particular implementation is considered, providing a hinge that is 135 mm long, 30 mm high and 45 mm wide, with a deployment moment varying between 0.1 and 0.3 Nm and a locking moment of 13 Nm. Stiffness tests have been carried out on the hinge, in the deployed configuration, and it is shown that the six stiffness coefficients can be estimated using simple analytical models. The moment versus rotation profile of the hinge is shown along with the results found from a finite-element simulation. The results of deployment testing, including shock imparted upon latching of the hinge, are presented for hinges with a variety of damping mechanisms.

Introduction

A number of space based deployable structures that are being developed at present, such as membrane synthetic aperture radars and ultra-high power solar arrays, involve the use of stiff members connected by self-locking hinges. The design of such frames can be simplified and their cost greatly reduced by the use of continuous, elastic connections, instead of standard mechanical hinges.

This paper presents a new design for a Tape-Spring Rolling (TSR) hinge, see Figure 1, which is a combination of steel tape-springs, mainly providing the deployment and locking moments, and a rolling hinge consisting of two sets of "wheels" held together by wires wrapped around them. These wires are held within grooves cut into the body of the wheels and are free to pass from one wheel to the other when the wheels are rotated. This very low friction arrangement is sometimes known as a "rolamite hinge" (Chironis and Sclater, 1996), and has well-defined kinematic properties. Note that there is no sliding, only rolling contact, and that the kinematic behaviour of the hinge is determined only by those parts of the rolamite wheels which come into contact; the rest of the wheel can have an arbitrary shape.

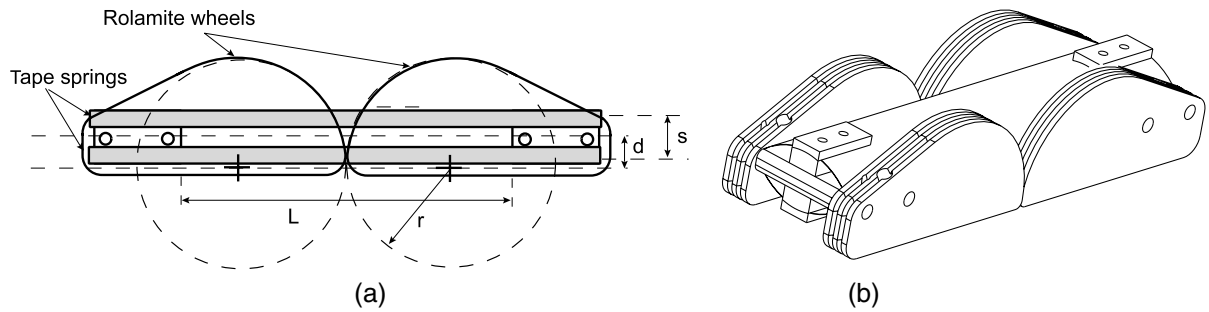

Figure 1: TSR Hinge.

The proposed design can be readily tailored to meet different applications and, in particular, is more compact and lighter than earlier designs. The stiffness, moment-rotation properties, and damping behaviour have been characterized and are presented in this paper.

[1] Department of Engineering, University of Cambridge. amw33@eng.cam.ac.uk.
[2] Department of Engineering, University of Cambridge, Cambridge CB2 1PZ, UK. pellegrino@eng.cam.ac.uk.

Proceedings of the 36 Aerospace Mechanisms Symposium, Glenn Research Center, May 15-17, 2002

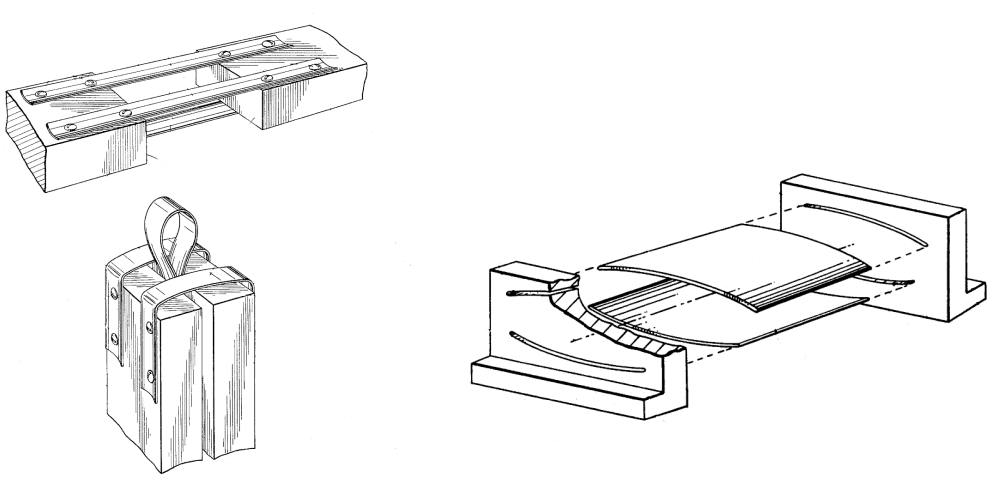

(a) (b)

Figure 2: Configurations of tape-spring hinges.

Review of Related Hinge Designs

Simple, self-actuating, self-locking hinges have been developed for a number of years for use as the deployment mechanisms for solar array panels, synthetic aperture radars (SARs), booms, radiators and the like.

Several successful designs have made use of curved elastic elements (tape-springs). Tape-spring hinges offer a number of benefits over standard hinges involving relative motion between rigid mechanical parts, that make them particularly suitable for use in deployable space structures:

- Zero friction and backlash.
- Elastic latching into locked position, giving highly repeatable and accurate positioning.
- No moving parts to jam or bind due to long-term storage or adverse environmental conditions.
- Simple manufacture and low cost.

Vyvyan (1968), Figure 2(a), patented a method of increasing the locking moment produced by a tape-spring hinge by placing the tape-springs in a parallel configuration, hence putting them in overall compression and tension rather than bending. An alternate arrangement is shown in Figure 2(b) (Chiappetta et al., 1993) where, unlike Figure 2(a), the tape-springs come into contact upon folding.

A major disadvantage inherent in the use of tape-spring hinges is that they have very low stiffness in the folded configuration. This can cause uncertainties in deployment and makes gravity compensation during ground testing problematic.

Aerospatiale (Auternaud et al., 1992) proposed a solution to this drawback by attaching a rolling hinge to the tape-spring, as shown in Figure 3. A functionally similar design has been manufactured by TRW Astro. Both designs provide better deployment control than the previous hinges, however both of these hinges were developed primarily for solar array panels, and hence are too wide for many other applications. Also, the Aerospatiale hinge is heavy (1.17 kg) and complex, whereas the locking stiffness of the TRW Astro hinge is expected to be quite limited.

A rolling hinge was developed by Hilberry et al. (1976), Figure 4, and functions by holding two rolling surfaces in contact by means of tensioned bands. As the hinge rotates, the bands pass from one rolling surface to

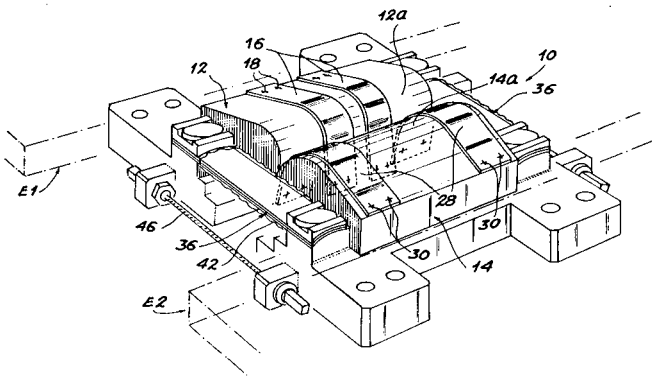

Figure 3: Aerospatiale hinge.

the other and their curvatures change signs. There is therefore no sliding contact within this hinge, thus making friction very low and removing the need for lubrication.

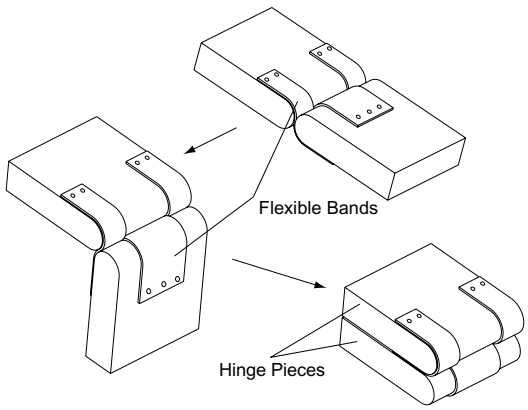

Figure 4: Rolling hinge.

Hilberry et al. (1976) also describe how the performance of a rolling hinge can be improved by changing the profile of the rolling surfaces or of the surfaces supporting the tension bands. For instance, the force pulling the two halves of the hinge together is increased if the bands run on a surface with a smaller radius than the rolling surface, Figure 5(a). Alternatively by making some of the tension band surfaces smaller than the others, as in Figure 5(b), a restoring moment is created upon rolling the hinge in the direction shown.

New Hinge Design

The new hinge design, first presented in Pellegrino et al. (2000), introduces two fundamental design changes:

- A double tape-spring is used. This produces a higher deployed bending stiffness and a much higher locking moment, both of which can be tailored to any particular application by varying the spacing of the tapes. Thus the complex locking mechanism of the Aerospatiale hinge is no longer required.

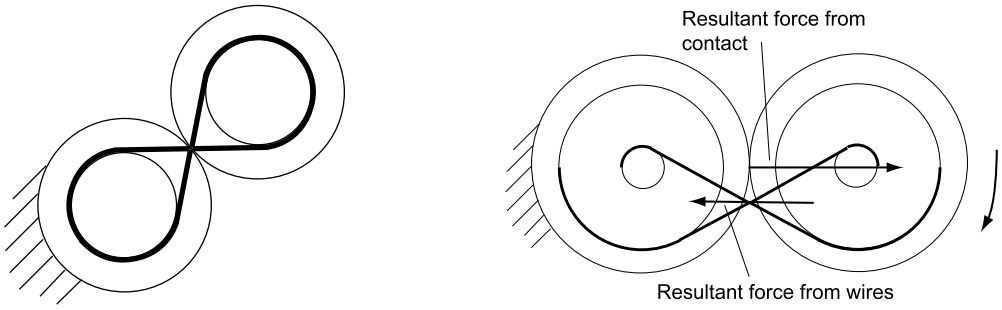

Figure 5: Alternative forms of rolling hinge.

- Steel bands in the rolling hinge are replaced by wires. This reduces the overall width of the mechanism and hence its weight, and allows a much simpler and more efficient wire tightening mechanism to be utilised.

The main geometric characteristics of the hinge are defined in Figure 1 and are as follows:

- The length, L, of the tape-springs, measured between the ends of the clamps.
- The separation distance, s, between the tapes, i.e. the distance between the neutral axes of the two springs.
- The offset distance, d, between the centre-line through the tape-springs and the centre-line through the rolamite wheels.
- The radius, r, of the rolamite wheels.

The particular TSR hinge that is investigated in this paper has L = 88 mm, s = 12.5 mm, d = 11 mm and r = 28.1 mm giving overall dimensions of 135 mm by 45 mm by 30 mm. It weighs 0.11 kg including all connections. The dimensions of the hinge are constrained by the requirement that the tape-springs should not be damaged during folding/unfolding. The smallest hinge that has been constructed with the same tape-springs has dimensions of 106 mm by 44 mm by 21 mm.

The new TSR hinge can be seen in Figure 6. The main parts of the rolling hinge are manufactured from 8 mm thick Delrin (a space-qualified Acetyl Resin) plate. Aluminium-alloy blocks connect the rolling parts to the tape springs. Nylon coated, 1 mm diameter stainless steel wire terminated by crimped aluminium tubes is used to hold together the rolling parts; tension adjustment is provided at one end by the wire passing through a screw with a lock-nut on the end. The prestress in the wires is sufficiently large that compressive contact between the rolamite wheels is always maintained. The tape-springs are cut from 25.4 mm wide, 0.1 mm thick, transverse radius 15 mm, "Contractor Grade" steel tape-measure, supplied by Sears Roebuck and Co.

TSR hinges with two or even three stacked tape springs also work well, and both the deployment and locking moments increase roughly proportionally, but note that the hinge described in this paper is made from a single pair of tape springs.

Deployed Stiffness

In order to estimate the natural frequency and stiffness of a structure utilising TSR hinges, the linear stiffnesses (K_{xx}, K_{yy} and K_{zz}) and the rotational stiffnesses (T_{xx}, T_{yy} and T_{zz}) of the hinge are required; the directions of x, y and z are defined in Figure 6. The stiffnesses of the component parts of a hinge were both

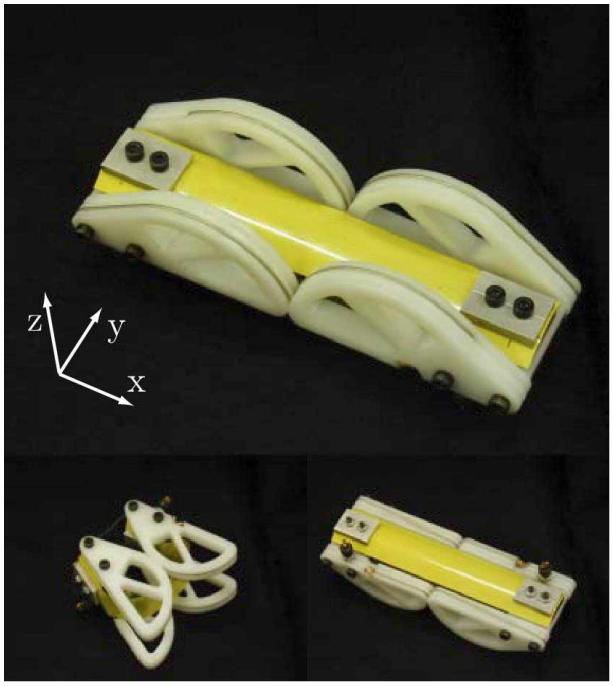

Figure 6: TSR hinge.

measured and predicted with various linear elastic analytical and finite element models. A summary of all the test results and analytical predictions is given in Table 1. The test results for the overall stiffness of the hinge in each component direction can be seen in Figure 7.

Table 1: Summary of Stiffness Results.

	Experiments			Predictions			
Direction	rolamite	Tape	Total	rolamite	Tape	Total	Units
K_{xx}	1768	5400	7223	1272	12172	13442	N/mm
K_{yy}	31.9	236	221	47	702	749	N/mm
K_{zz}	115	9.66	134	72	33	106	N/mm
T_{xx}	40	29	75	45	54	99	kNmm/rad
T_{yy}	0	228	480[a]	0	475	614	kNmm/rad
T_{zz}	360	480	782	779	453	1232	kNmm/rad

[a] This particular value was measured on a hinge with d =4.5 mm.

Analytical predictions for the stiffnesses were obtained using the expressions given below. Note that each equation contains two separate terms, which correspond to the rolamite and tape-spring stiffness contributions, respectively. The definition and numerical value given to each term in these expressions are listed in Table 2. The finite element predictions were slightly more accurate, but are not presented here because they are much harder to obtain and cannot be readily transferred to other hinge designs.

The axial stiffness, K_{xx}, was predicted by modelling the rolamite (subscript r) part of the hinge with two equivalent beams whose axial stiffness takes into account the compliance of the hertzian contact between the pairs of wheels (Johnson, 1987); the tape-springs (subscript t) were also modelled as two beams:

$$K_{xx} = \left[\frac{L}{2b_r d_r E_r} + \frac{4}{\pi w E_r^*} \left(\ln \frac{4\pi r w E_r^*}{Q_r} - 1 \right) \right]^{-1} + \frac{2A_t E_t}{L} \tag{1}$$

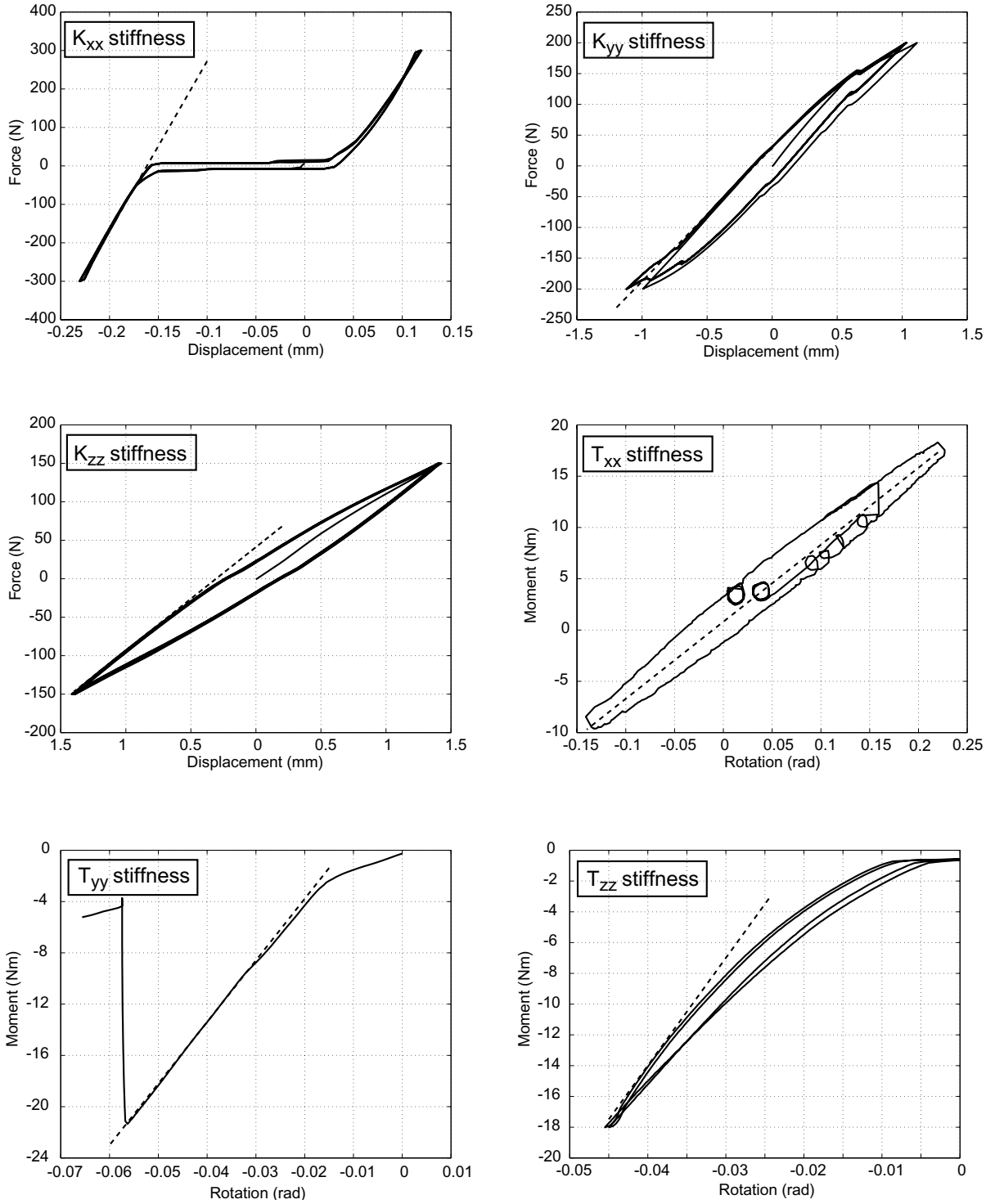

Figure 7: Hinge response in six stiffness tests.

Here Q_r is the contact force, whose value does not significantly affect the results in the range considered.

The in-plane shear stiffness, K_{yy}, and the out of plane shear stiffness, K_{zz}, were predicted by considering the rolamite and tape-spring parts of the hinge as two separate built-in beams. Hence:

$$K_{yy} = 2\frac{E_r b_r d_r^3}{L^3} + 2\frac{12 E_t I_{zz}}{L^3} \tag{2}$$

$$K_{zz} = 2\frac{E_r b_r^3 d_r}{L^3} + 2\frac{12 E_t I_{yy}}{L^3} \tag{3}$$

The torsional stiffness, T_{xx}, was predicted by considering the end deflections, in the z-direction for the rolamite and the y-direction for the tapes, induced by a unit torsional rotation of the hinge. Each deflection causes associated shear forces in the equivalent beams defined above, from which the required twisting moment is:

$$T_{xx} = 2\frac{E_r b_r^3 d_r h^2}{2L^3} + 2\frac{12 h^2 E_t I_{zz}}{2L^3} \tag{4}$$

The in-plane bending stiffness, T_{yy}, was predicted by considering that a unit rotation about y causes extension and compression of the tape-springs. The rolamite has zero stiffness on its own, as this is the direction of free rotation, but it provides an elastic constraint for the tape springs acting as a single beam, which leads to an additional stiffness contribution. Hence T_{yy} is:

$$T_{yy} = \left[\frac{L}{2b_r d_r E_r} + \frac{4}{\pi w E_r^*}\left(\ln\frac{4\pi r w E_r^*}{Q_r} - 1\right) + \left(\frac{2A_t E_t}{L}\right)^{-1}\right]^{-1} d^2 + \frac{A_t E_t s^2}{2L} \tag{5}$$

The out-of-plane bending stiffness, T_{zz}, was predicted by considering that a unit rotation about z puts a pair of rolamite wheels into tension and the other pair into compression, whilst the tape-spring was considered as a built-in beam subject to an end rotation. The resulting expression is:

$$T_{zz} = \frac{d_r^2}{2}\left[\frac{L}{2b_r d_r E_r} + \frac{4}{\pi w E_r^*}\left(\ln\frac{4\pi r w E_r^*}{Q_r} - 1\right)\right]^{-1} + 2\frac{E_t I_{zz}}{L} \tag{6}$$

Moment-Rotation Properties

The moment-rotation relationship of TSR hinges is required in order to model the dynamic deployment of any system utilising these hinges. Seffen and Pellegrino (1999) have developed analytical expressions for the key parameters determining the moment-rotation behaviour of tape-springs. From these expressions, the "steady-state" deployment moment of a TSR hinge with a single pair of tape springs is given by:

$$M = \frac{E_t t^3 \alpha}{6(1-\nu^2)} \tag{7}$$

Where t and ν are the thickness and Poisson's ratio, respectively, of a tape spring and α the angle subtended by its cross-section, in radians. Note that this expression does not include the effects of contact between the two tape springs and of the constraint imposed by the rolamite wheels; hence the actual deployment moment is usually larger and also non-uniform.

Greater accuracy requires a fully non-linear numerical formulation to be adopted. Hence, a quasi-static simulation of the folding of a TSR hinge was made with the finite-element package Abaqus (Hibbit et al. 2000). The purpose of the FE modelling was to accurately simulate the snap-through deformation of the

Table 2: Terms used in Analytical Expressions.

Term	Definition	Value	Units
A_t	cross-sectional area of tape	2.5	mm
b_r	width of equivalent rolamite beam (z direction)	10	mm
d	centre-to-centre distance between rolamite wheels and tape spring	11	mm
d_r	depth of equivalent rolamite beam (y direction)	8	mm
E_r	Young's modulus of rolamite wheels (Delrin)	3.1	kN/mm^2
E_r^*	contact modulus (= $E/2(1-\nu^2)$)	1.6	kN/mm^2
E_t	Young's modulus of tape (steel)	210	kN/mm^2
h	width of rolamite hinge	35	mm
I_{yyt}	2nd moment of area for one tape (y-axis)	95	mm^4
I_{zzt}	2nd moment of area for one tape (z-axis)	95	mm^4
L	length of tape and equivalent rolamite beam	88	mm
Q_r	contact force between rolamite wheels	20-800	N
r	radius of rolamite wheels	28.1	mm
s	separation of tape neutral axes	12.5	mm
w	width of rolamite contact area	10	mm

tape springs and to derive the full bending moment-rotation relationship of the hinge, including the buckling moment.

Therefore, a full 3D model was set up, Figure 8. The tape springs were modelled using 50 $\times$ 12, 4-node doubly curved general-purpose shell elements (s4) for each spring. These elements were generated with logarithmic bias along the tape length so that the finer mesh is concentrated in the middle of the tapes, where most of the deformation before the snap and the contact between the tapes take place.

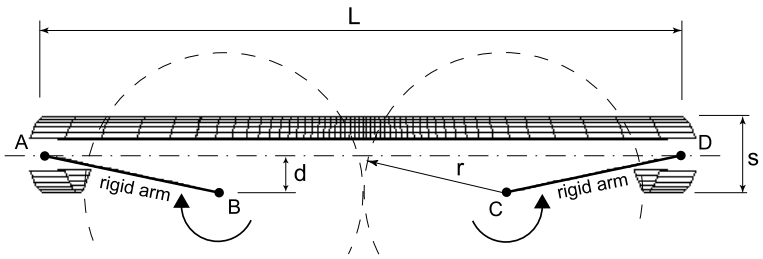

Figure 8: Finite element model of TSR hinge.

The rolling part of the TSR hinge was modelled as a set of two rigid arms, using rigid beam elements. The arms connect the centres of rotation, B and C, to nodes A and D, and multi-point constraints were defined between these nodes and the nodes at the end of the tapes. Nodes B and C are fixed in all directions and can only rotate around an axis parallel to y. In order to simulate the hinge deformation, equal clockwise and anti-clockwise rotations of up to 90 deg. were applied to nodes B and C, respectively. Contact between the tapes was modelled as a surface to surface contact.

The Riks solution procedure was initially chosen, in order to trace the complete equilibrium path of the hinge, including unstable parts. However, there were problems with convergence after the first snap-through point, hence a rotation controlled solution procedure had to be adopted instead. The "Stabilise" function available in Abaqus was used, which automatically switches to a pseudo-dynamic simulation when an instability is detected. This method gave the desired convergence, but it should be noted that unstable parts of the response cannot be predicted by this method.

The finite element predictions were validated against experimental results obtained from an ESH Torsion

Machine. Figure 9(a) shows the testing arrangement; the head of the testing machine applies a rotation to the centre of one of the rolamite wheels, whilst measuring the moment, and the centre of the other wheel is held in a bearing coaxial with the wheel. The measured response of the hinge during folding and unfolding has been plotted in Figure 9(b) along with the FE predictions. The measured peak buckling moment —not shown in the figure— was 13 Nm, which compares with a prediction of 19 Nm. However, during *deployment* the maximum moment was 1 Nm, much lower than the 12 Nm predicted by the FE simulation.

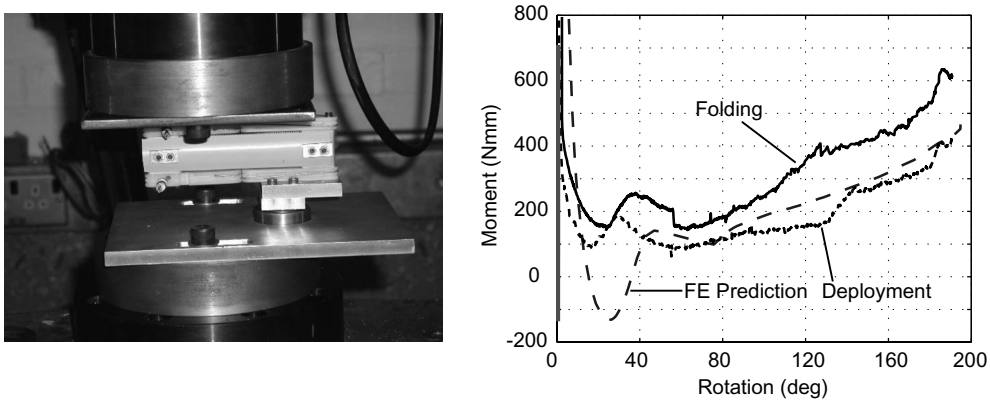

(a) (b)

Figure 9: Moment-rotation test set-up and results.

Damping

Damping can have two functions in a hinge; to slow the time required for deployment and to reduce the shock arising from locking. In order to test the effectiveness of different damping methods, a mock-up of a deployable panel system on a satellite was made from two identical aluminium honeycomb panels. Panel 1 is attached to a rigid base; panel 2 is connected to panel 1 by two identical TSR hinges. Each panel has dimensions of 1 m by 0.5 m, and weighs 1.67 kg including hinges and hinge fittings. The whole set up is shown in Figure 10.

Deployment tests were conducted for three different damping configurations, as shown below:

1. No additional damping.
2. Two brown Oasis foam blocks placed between the two panels, as shown in Figure 11(a), to absorb energy by crushing the foam during the final approach phase.
3. Single layer of 3M 434 sound damping tape applied to both sides of each tape spring, as shown in Figure 11(b).

Deployment Tests

The deployment of the panel was recorded using a Kodak EKTAPRO HS 4540 high speed video camera and digitised to obtain rotation vs. time graphs. The results can be seen in Figure 12 for case 1 (undamped) and case 3. Case 2 gives exactly the same results as case 1, as the foam does not affect the large-scale rotation behaviour. It can be seen that the damping layers make a negligible difference to the rotation vs. time response.

A model of the deployment of the panel was made using Pro/Mechanica Motion (Parametric Technology Corp., 2001), a rigid body dynamic analysis program. The loads applied to this model were those found

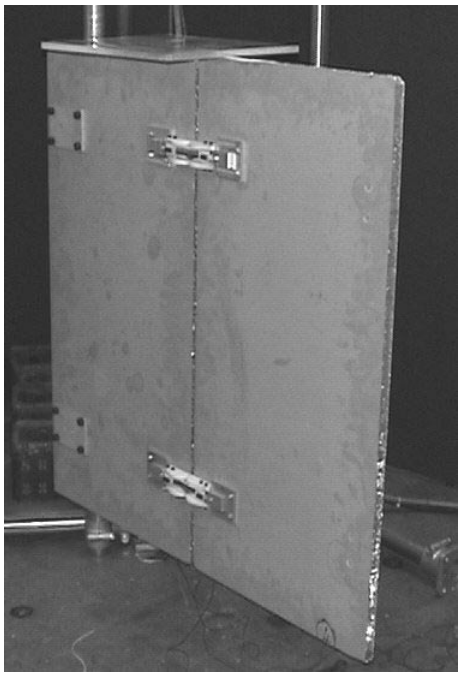

Figure 10: Deployable panel.

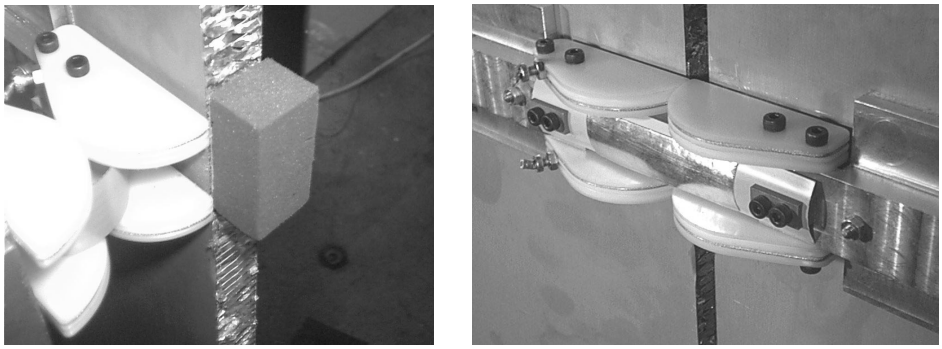

(a) (b)

Figure 11: Damping foam and damping tape.

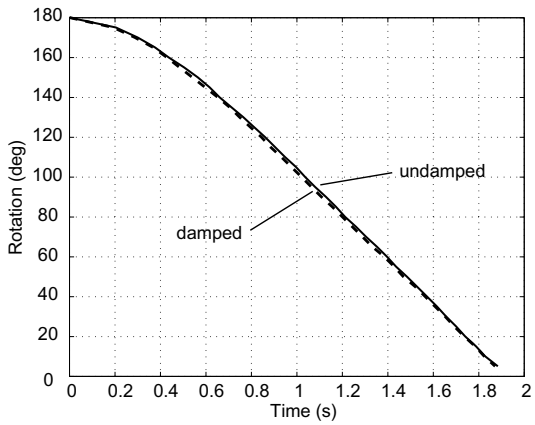

Figure 12: Deployment of panel with damped and undamped hinges.

from the Abaqus model of the hinge, taking into account the direction of motion and the state —i.e. fully unfolded or not— of the hinge.

The rotation vs. time results from this model can be seen in Figure 13 along with the results from the undamped test. The deployment is modelled with good accuracy up to the point of locking, but subsequently the simulation shows the hinge unlocking and rotating back to a rotation of around 20° and then oscillating backwards and forwards a number of times, before finally locking. Note that the current hinge design can turn only in one direction, and hence in the opposite direction it is able to resist a very large moment.

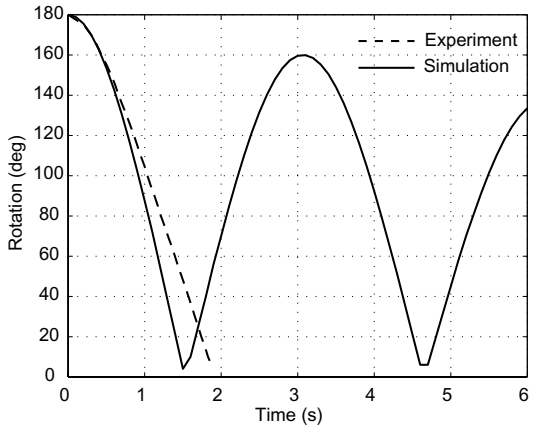

Figure 13: Comparison of rotation vs. time response to Pro/Mechanica simulation.

This difference in the post-locking behaviour could be due to a number of factors, such as:

- Damping within hinge. At locking there could be significant damping present due to stretching of the wires, compression of the hinge wheels, stretching of the tapes or slipping of the connections.
- Energy loss due to buckling.
- Incorrect modelling of the moment-rotation properties of the hinge where the moment-rotation properties of the hinge vary from those predicted by the Abaqus analysis.
- Resistance during panel deployment. This resistance could arise due to friction within the hinge or air resistance on the panel.

Shock Measurements

In addition to measuring the rotation of panel 2, four accelerometers were attached to the apparatus, two to each panel, in the positions shown in Figure 14. The distance from the hinge attachment to the accelerometers was minimised to measure the peak shock levels. The accelerometer outputs were logged at 5000 Hz using a PC with an analogue to digital converter board and a program written in Labview (National Instruments, 1998).

The shock resulting from deployment of a panel with hinges without additional damping can be seen in Figure 15. The hinges do not lock fully on first deployment but re-buckle twice; hence a total of three acceleration peaks can be seen in the plots, each corresponding to the tape springs snapping into the deployed configuration. The maximum acceleration is approximately 1500 m/s^2 (150 g) and there is little difference between accelerations in different directions.

The shock resulting from deployment of a panel with two 12 mm long pieces of Oasis foam can be seen in Figure 16. The size of the foam blocks was determined by setting the kinetic energy of the system on latch-up (equal to the strain energy in the hinges, given by the area under the moment-rotation graph) equal

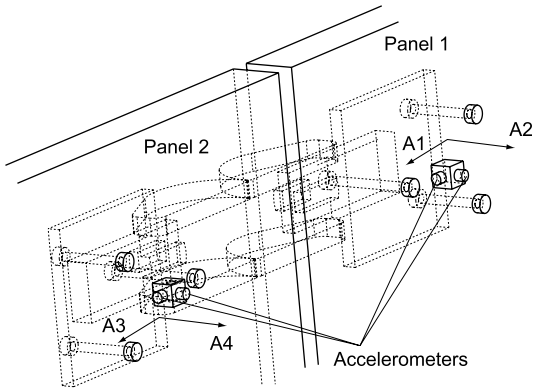

Figure 14: Accelerometer positioning.

to the energy required to crush the foam to a size that allows full deployment of the panel. The panel now locks the first time, without re-buckling the tape-spring hinges, and the maximum acceleration is reduced to approximately 600 m/s^2 (60g). Successful deployment of the panel was found to be very sensitive to the length of the foam blocks used. For example, when the length was increased to 12.5 mm the panel did not lock; ideally a larger piece of less dense foam with a lower crushing stress should be used.

The shock resulting from the deployment of a panel with 3M 434 sound damping tape attached to both sides of each tape-spring can be seen in Figure 17. The maximum shock is now around 250 m/s^2 (25g) in all directions.

Conclusions

The hinge presented in this paper is significantly lighter and smaller than previous designs. It also provides predictable moment-rotation and stiffness properties. It has been used as the deployment mechanism in full size verification models of SARs and Solar Panels.

The deployed stiffness properties of the hinge can be predicted analytically with good accuracy, and the equations that have been presented can be used to tailor the stiffness properties of the hinge to a given set of requirements.

Modelling the full moment-rotation relationship of the hinge with good accuracy has to take into account the effect of contact between the tapes, which was achieved with a finite element analysis. A relationship obtained thus has been used to successfully predict the deployment dynamics of a structure containing TSR hinges, however the prediction of the amount of energy dissipated within the hinge during latching is an area where further work is needed. From a practical view point, it has been found that the addition of damping tape is more effective at reducing shock than damping foam. Damping tape gives a six-fold reduction in the imparted shock over an undamped hinge. None of the damping systems tested have any effect on the large scale rotation-time properties.

Acknowledgments

The work presented in this paper was funded by the British National Space Centre and technically supported by ASTRIUM UK Ltd. We thank the technical monitor, Mark Roe, for advice and many valuable suggestions. Financial support from the Science and Engineering Research Council, in the form of a studentship for A.M.W. is gratefully acknowledged.

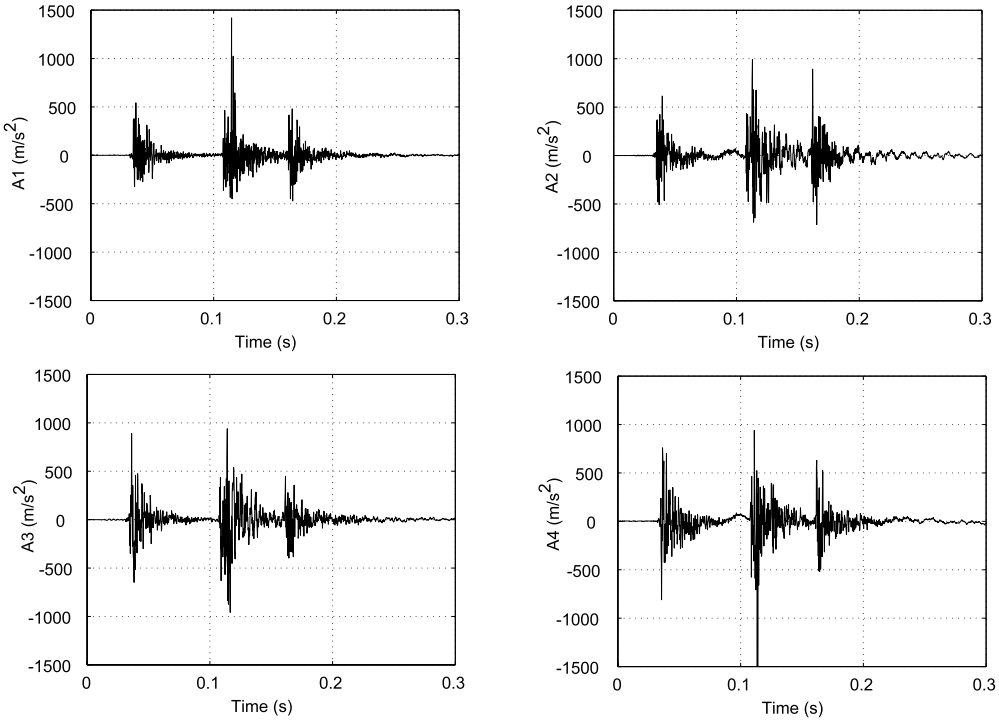

Figure 15: Locking shock for panel with no damping.

References

Auternaud, J. et al. (1992). Self motorized antifriction joint and an articulated assembly, such as a satellite solar panel equipped with such joints, U.S. Patent 5,086,541. February 11th, 1992.

Chiappetta F.R., Frame C.L., Johnson K.L. (1993). Hinge element and deployable structure including hinge element, U.S. Patent 5,239,793. August 31, 1993.

Chironis, N.P. and Sclater, N. (1996). Mechanisms and mechanical devices sourcebook. Second Edition, McGraw-Hill, New York.

Hibbit, Karlsson and Sorensen (2000). ABAQUS Version 6.1.0. Pawtucket, RI 02860.

Hilberry B.M. and Hall A.S. (1976). Rolling contact prosthetic knee koint, U.S. Patent 3,945,053. March 23rd, 1976.

Johnson, K.L. (1987). Contact Mechanics, Cambridge University Press, Cambridge.

National Instruments (1998). Labview Version 5.0.1.

Parametric Technology Corporation (2001). Pro/Mechanica 2001, 140 Kendrick St, Needham, MA 02494.

Pellegrino, S., Green, C., Guest, S.D. and Watt A. (2000). SAR Advanced Deployable Structure. CUED/D-STRUCT/TR191, Department of Engineering, University of Cambridge.

Seffen, K. A. and Pellegrino, S. (1999). Deployment dynamics of tape springs. Proceedings of the Royal Society of London, series A, **455**, 1003-1048.

Vyvyan, W.W. (1968). Self-actuating, self-locking hinge, U.S. Patent 3,386,128. June 4th 1968.

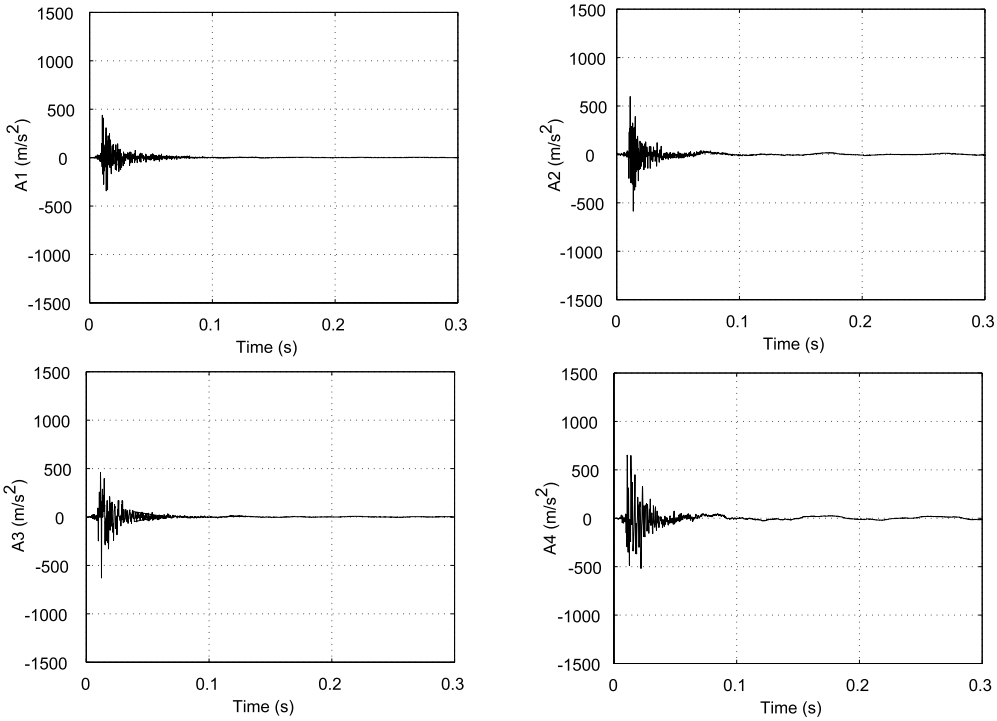

Figure 16: Locking shock for panel with 12 mm brown Oasis foam.

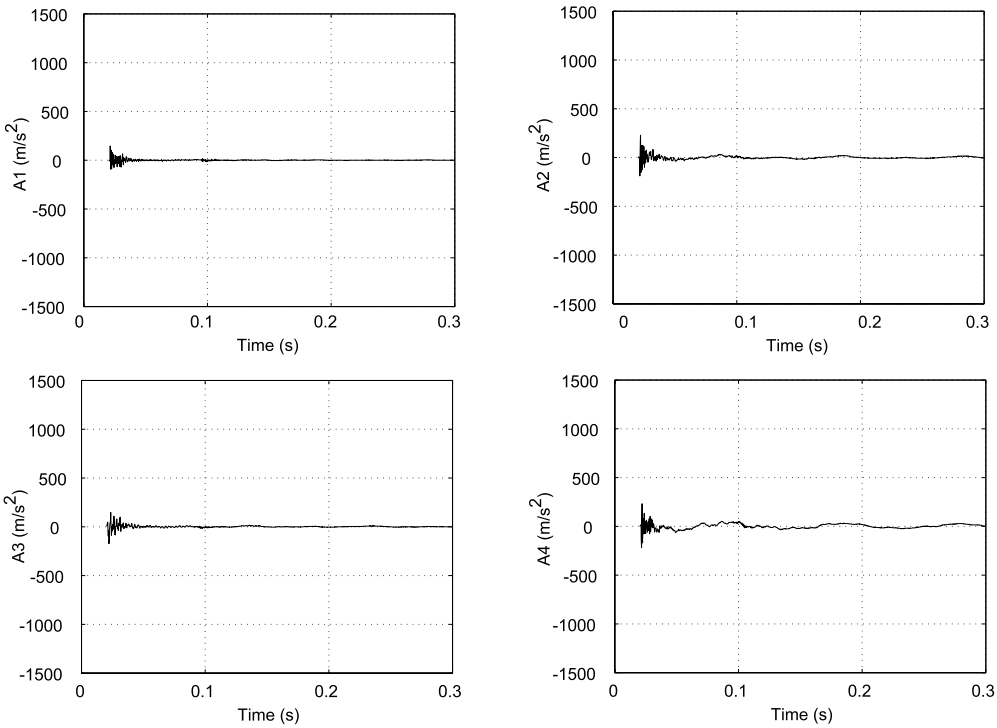

Figure 17: Locking shock for panel with 3M 434 sound damping tape.